# Role of Multi - detector row CT in the diagnosis and management of Solid Renal Masses

## Thesis submitted for partial fulfillment of MD Degree in Radiodiagnosis

Submitted by

#### Tamer Wahid Mahmoud Kassem

(M.B.B.Ch; M.Sc.)
Cairo University

Supervisors

#### Prof. Sameh Abdel Aziz Hanna

Professor of Radiodiagnosis Faculty of Medicine Cairo University

## Prof. Hesham Abdel Hamid Badawy

Professor of Urology Faculty of Medicine Cairo University

## Ass. Prof. Manal Halim Wahba

Assistant Prof. of Radiodiagnosis
Faculty of Medicine
Cairo University

Faculty of Medicine Cairo University 2009

#### **ABSTRACT**

Multiphasic MD row CT scan of the kidneys as a promising noninvasive technique for the assessment and characterization of different solid renal mases may replace other invasive techniques as angiography and avoid unnecessary repititive IV contrast injections. Its potential advantages in preoperative evaluation is providing accurate data regarding their positions, local infiltrations, venous involvement, renal vascular anatomy, regional lymph nodes and distant metastasis.

#### **KEY WORDS**

Multiphasic, Multidetector CT scan, Solid Renal Masses

## ACKNOWLEDGMENT

It a great pleasure to express my deep gratitude and thanks to Prof. Sameh Abdel Aziz Hanna Professor of Radiodiagnosis Faculty of Medicine Cairo University for his very constructive and meticulous supervision of this work. His continuous and stimulating wise comments were very valuable.

Many thanks and gratefulness are also forwarded to Prof. Hesham Abdel Hamid Badawy Professor of Urology Faculty of Medicine Cairo University for his support and real cooperation.

I am deeply thankful and indebted to A. Prof. Manal Halim Wahba Assistant Professor of Radiodiagnosis Faculty of Medicine Cairo University.

To my wife and daughters:

I really appreciate your cooperation, understanding and help.

## LIST OF ABBREVIATIONS

AML Angiomyolipoma

AV Arterio-venous

CMP Corticomedullary phase

CT Computed tomography

CTA CT angiography

CTU CT urography

DAS Data acquisition system

EP Excretory phase

EU Excretory urography

F Female

HU Hounsfield unit

IVC Inferior vena cava

IVP Intra venous pyelography

IVU Intra venous urography

LN (s) Lymph node (s)

M Male

MDCT Multi detector row CT

MIP Maximum intensity projection

MR or MRI Magnetic resonance imaging

MSCT Multislice CT

NAD No abnormality detected

NHL Non Hodgkin's lymphoma

NP Nephrographic phase

PACS Picture archiving and communication system

RCC (s) Renal cell carcinoma (s)

ROI Region of interest

RV Renal vein

SC Sickle cell

SSD Surface shaded display

STD Standard deviation

TCC Transitional cell carcinoma

TSC Tuberous sclerosis complex

US Ultrasound

VR Volume rendering

XGP Xanthogranulomatous Pyelonephritis

3D Three dimensional

2D Two dimensional

## LIST OF FIGURES

Figure 1 Renal artery

Figure 2 Normal renal segmental arterial anatomy

Figure 3 Renal vein

Figure 4 MIP and VR CTA

Figure 5 Renal Vascular variants

Figure 6 TNM staging system for RCC

Figure 7 Phases of renal enhancement at MDCT

Figure 8 Incidental RCC

Figure 9 Normal collecting system and ureters

Figure 10 Combined CT and EU CTU technique

Figure 11	CT urographic MIP image
Figure 12	Schematic comparison of VR and MIP images
Figure 13	Schematic comparison of VR and MIP images after slap editing
Figure 14	Further slap editing
Figure 15	CMP and NP
Figure 16	RCC
Figure 17	RCC
Figure 18	Left sided RCC
Figure 19	Invasive papillary urothelial carcinoma
Figure 20	Invasive papillary urothelial carcinoma
Figure 21	Upper pole tumor
Figure 22	Tumor extension
Figure 23	RCC confined to the kidney (T1 and T2)
Figure 24	Perinephric spread of RCC (T3a)
Figure 25	False-negative finding of perinephric spread
Figure 26	False-positive finding of perinephric spread
Figure 27	RCC with extension into the left RV (T3b)
Figure 28	RCC with extension into RV and IVC (T3c)
Figure 29	RCC with extension into the left RV and intrahepatic portion of IVC (T3c)
Figure 30	RCC with tumoral extension into the supradiaphragmatic level of IVC (T4b)
Figure 31	Relationship of tumor to the collecting system
Figure 32	Tumor supply
Figure 33	Multiple renal veins.
Figure 34	RCC with enhancing retroperitoneal nodal metastases (N1-N3)
Figure 35	Large RCC with possible extension into the liver
Figure 36	Multiple renal cell carcinomas
Figure 37	Small RCC treated with nephron-sparing nephrectomy

Figure 38	RCC extending to the renal hilum.
Figure 39	Renal pseudotumor due to respiratory misregistration
Figure 40	Extension of RCC into the renal sinus
Figure 41	Sporadic bilateral synchronous multifocal RCC
Figure 42	Contralateral adrenal metastasis from RCC
Figure 43	RCC associated with bulky NHL
Figure 44	Paraaortic LN metastasis from an undetected RCC
Figure 45	AV fistula within a renal tumor
Figure 46	Spontaneous perirenal hematoma
Figure 47	RCC engulfing perirenal fat.
Figure 48	Transparenchymal renal propagation and RV thrombosis
Figure 49	Collecting duct carcinoma
Figure 50	Clear cell sarcoma of the kidney
Figure 51	Renal medullary carcinoma
Figure 52	Renal oncocytoma
Figure 53	Wilms tumor
Figure 54	Rhabdoid tumor
Figure 55	Malignant rhabdoid tumors of the kidney
Figure 56	Nephroblastomatosis
Figure 57	Mesoblastic nephroma
Figure 58	Renal angiomyolipoma
Figure 59	AML with minimal fat
Figure 60	RCC
Figure 61	RCC
Figure 62	AML with minimal fat.
Figure 63	Ruptured AML.
Figure 64	Angiomyolipoma
Figure 65	Undifferentiated renal sarcoma
Figure 66	Clear cell sarcoma
Figure 67	TCC

Figure 68	TCC of the renal pelvis
Figure 69	TCC
Figure 70	Drawing: multiple masses in renal lymphoma
Figure 71	Large B-cell lymphoma
Figure 72	Large cell lymphoma
Figure 73	Drawing: dominant lymphomatous renal mass
Figure 74	Renal lymphoma
Figure 75	Large B-cell lymphoma
Figure 76	Drawing: bulky retroperitoneal mass invading the renal hilum and enveloping the renal vessels
Figure 77	Diffuse lymphocytic lymphoma
Figure 78	Drawing: isolated perirenal lymphoma
Figure 79	Perirenal soft-tissue mass
Figure 80	Large cell lymphoma
Figure 81	Drawing: infiltrative lymphoma
Figure 82	Primary renal lymphoma
Figure 83	Infiltrative renal lymphoma
Figure 84	B-cell lymphoma
Figure 85	NHL
Figure 86	Diffuse large cell lymphoma
Figure 87	Pyelonephritis
Figure 88	Renal abscess
Figure 89	Renal mass incidentally found
Figure 90	Left renal pseudotumor
Figure 91	Illustration shows ball-versus-bean concept
Figure 92	Polar nephrectomy

## LIST OF CHARTS

Chart 1	Male to Female ratio
Chart 2	46 cases are unilateral and 4 cases are bilateral
Chart 3	Different pathologies encountered in the study
Chart 4	Mean age in different pathologies
Chart 5	Percentage of benign and malignant cases in the study
Chart 6	Benign cases in the study
Chart 7	Malignant cases in the study
Chart 8	Unilateral and bilateral affection in different pathologies
Chart 9	Male to female ratio in different pathologies
Chart 10	Lymph nodal metastasis, renal vein and IVC thrombosis and distant metastatic spread in different pathologies
Chart 11	Pattern of enhancement in RCC cases
Chart 12	Pattern of enhancement in TCC cases
Chart 13	TNM staging in RCC cases

Table 1 Technique of Multiphasic CT Study For Renal Masses.

## TABLE OF CONTENTS

•	List of appreviations	
•	List of figures	П
•	List of charts	VI
•	Introduction and Aim of work	1
•	Review of Literature	
	Anatomy	2
	Pathology	8
	Technique	30
	<ul> <li>Multiphasic CT study of a renal mass</li> </ul>	49
•	Patients and methods	113
•	Results	118
•	Case presentation	129
•	Discussion	165
•	Conclusion	178
•	Summary	180
•	References	182
•	Arabic summary	196

#### INTRODUCTION

The role of computed tomography (CT) in the evaluation of renal lesions is very well-known. CT is widely accepted as the preferred imaging technique for suspected renal tumors, and also has an important role in tumor staging. Benign renal processes, including cystic disease, renal infection, and benign tumors may simulate malignant renal tumors, and could be defined correctly by CT. The improvements in CT technique and increased use of cross-sectional imaging have facilitated the detection of small or previously undiagnosed renal masses. Helical CT technology further improved renal imaging volume-averaging artifacts, with decreasing eliminating respiratory misregistration artifacts and allowing image acquisition during the peak intravenous contrast enhancement. Helical CT image acquisition has also led to improved data sets available for three-dimensional imaging.

To date, the major role of three-dimensional (3D) CT imaging for renal pathology has concentrated on the non-invasive evaluation of renal artery stenosis and other renal vascular abnormalities and recently literature reveals a large number of studies that describe the use of 3D-CT imaging and 3D-CT angiography (CTA) in renal mass evaluation.

#### **AIM OF WORK**

The aim of this study was to investigate the efficacy of multiphasic CT, 3D-CT imaging, CTA and CTU in the demonstration of anatomy and characterization of nature of renal masses during the preoperative evaluation.

## **Gross Anatomy**

An average adult kidney weighs about 160 grams. It is 12 cm in length, 6 cm in breadth and 3 cm in thickness and lies on the posterior abdominal wall in the para-vertebral gutter. The exact position of the kidneys varies with respiration and the position of the body, but they lie approximately opposite the three upper lumbar vertebrae. The left kidney lies a little higher than the right. The posterior surface of each kidney faces postero-medially and the anterior surface faces antero-laterally. Its convex border faces outward and the concave border inward. It is important to remember this oblique position when radiographs are viewed (Hall-Craggs, 1985).

The kidney and its vessels are embedded in peri-renal fat, which is thickest at the renal borders, and prolonged at the hilum into the renal sinus. Fibrous connective tissue surrounding this fat is condensed as the renal fascia (Gerota's fascia). The anterior layer of the renal fascia extends medially in front of the kidney and its vessels. The posterior layer passes medially between the kidney and the fascia on the quadratus lumborum and psoas major muscles, attaching to it at the lateral and medial borders of the psoas. It also attaches to the vertebrae and inter-vertebral discs (Williams et al., 1995).

Medially, the anterior and posterior layers do not form a well defined anatomic boundary, but fuse with the adventitia of the aorta and inferior vena cava. At the lateral renal borders, the two layers of renal fascia fuse to form the lateroconal fascia, which separates the peri-renal fat from the flank fat *(Lee et al., 1983)*. Superiorly, the two layers of renal fascia fuse above the suprarenal gland, while, below the kidney, the two layers are not firmly adherent together *(Williams et al., 1995)*.

At the level of the kidneys, the retroperitoneum is divided into three spaces, the anterior para-renal, the peri-renal, and the posterior para-renal spaces (Lee et al., 1983).

The anterior para-renal space extends from the posterior parietal peritoneum anteriorly, to the anterior renal fascia posteriorly. This space contains the pancreas, the duodenum, the descending and ascending colon. The anterior para-renal spaces are continuous across the midline *(Harell, 1985)*.

The peri-renal space is bounded anteriorly by the anterior renal fascia, and posteriorly, by the posterior renal fascia. It contains a variable quantity of fat, the kidney, adrenal and the proximal ureter (Harell, 1985).

The posterior pararenal space extends from the posterior renal fascia to the fascia overlying the quadratus lumborum and the psoas muscle. It has a variable medial extent and is open laterally towards the flank. It contains no retroperitoneal organs *(Harell, 1985)*.

#### **Renal Structure**

The cortex is the outer region. It lies immediately beneath the capsule and extends inward as the renal columns of Bertin. The cortex is about 1 cm in thickness. It is well vascularized and envelops the renal pyramids. The medulla, the inner region, is made up of several conical structures (up to 18 medullary pyramids may be present). The bases of the pyramids are located at the cortico-medullary junction and the apices extend into the hilum of the kidney as the papillae. Each papilla is "grasped" by a hollow minor calyx. The minor calyces are the branches of 3-4 major calyces, which communicate to form the renal pelvis. Urine that flows from the papillae is collected in the pelvis and passes to the bladder through the ureters (Hall-Craggs, 1985 and Andreoli et al., 1993).

## **Normal Renal Vascular Anatomy**

#### **Renal Arteries**

In most individuals, each kidney is supplied by a single renal artery that originates from the abdominal aorta. The renal arteries typically arise from the aorta at the level of L2 below the origin of the superior mesenteric artery, with the renal vein being anterior to the renal artery. The renal arteries course anterior to the renal pelvis before they enter the medial aspect of the renal hilum. The right renal artery typically demonstrates a long downward course to the relatively inferior right kidney, traversing behind the inferior vena cava (Kadir S, 1991). Conversely the left renal artery, which arises below the right renal artery and has a more horizontal orientation, has a rather direct upward course to the superiorly positioned left kidney. Both renal arteries usually course in a slightly posterior direction because of the position of the kidneys (Dyer R, 1993) and (El-Galley and Keane, 2000).

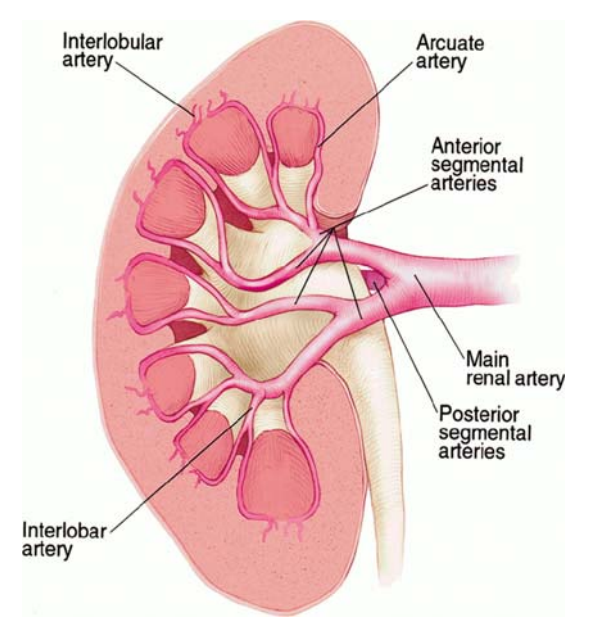


Figure 1. Renal artery (Bruce et al. 2001).

The main renal artery divides into segmental arteries near the renal hilum. The first division is typically the posterior branch, which arises just before the renal hilum and passes posterior to the renal pelvis to supply a large portion of the blood flow to the

4

posterior portion of the kidney. The main renal artery then continues before the dividing into four anterior branches at the renal hilum: the apical, upper, middle and lower anterior segmental arteries. The apical and lower anterior segmental arteries supply the anterior and posterior surfaces of the upper and lower renal poles, respectively; the upper and middle segmental arteries supply the remainder of the anterior surface. The segmental arteries then course through the renal sinus and branch into the lobar arteries. Further divisions include the interlobar, arcuate and interlobular arteries. Depiction of the relatively avascular plane between the anterior and posterior arterial divisions of the kidney is important to the surgeon, because the site can be used for a clean incision toward the renal pelvis at the time of surgery. The site is usually located posteriorly, one-third of the distance between the posterior and anterior kidney surfaces. A similar avascular plane exists between the posterior renal segment and the polar renal segments (Bruce et al., 2001).

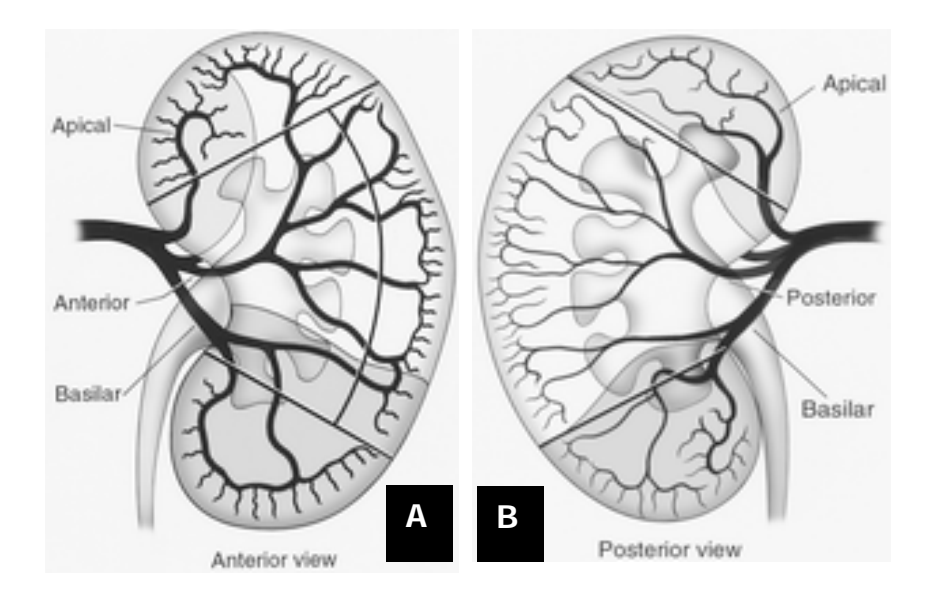


Figure 2. Normal renal segmental arterial anatomy. Drawings of the kidney from an anterior (A) and posterior (B) perspective demonstrate the apical, anterior, posterior, and basilar branches of the renal artery. (Deirdre et al., 2000)

#### **Renal veins**

The renal cortex is drained sequentially by the arcuate veins and interlobar veins. The lobar veins join to form the main renal vein. The renal vein usually lies anterior to the renal artery at the renal hilum. The left renal vein is almost three times longer than the right renal vein. The left renal vein averages 6-10 cm in length and